
The Sandbox Environment for Generalizable Agent Research (SEGAR)

R Devon Hjelm^{1 2 3 *} Bogdan Mazoure^{4 2 *} Florian Golemo²
 Felipe Vieira Frujeri⁵ Mihai Jalobeanu⁶ Andrey Kolobov⁶

Abstract

A broad challenge of research on generalization for sequential decision-making tasks in interactive environments is designing benchmarks that clearly landmark progress. While there has been notable headway, current benchmarks either do not provide suitable exposure nor intuitive control of the underlying factors, are not easy-to-implement, customizable, or extensible, or are computationally expensive to run. We built the Sandbox Environment for Generalizable Agent Research (SEGAR) with all of these things in mind. SEGAR improves the ease and accountability of generalization research in RL, as generalization objectives can be easily designed by specifying task distributions, which in turn allows the researcher to measure the nature of the generalization objective. We present an overview of SEGAR and how it contributes to these goals, as well as experiments that demonstrate a few types of research questions SEGAR can help answer.

1. Introduction

Consider the problem of training an automated agent to perform a set of sequential decision-making tasks in a real-world setting, such as autonomous driving (Kendall et al., 2019) or robotic control (Levine et al., 2016). This agent should take a correct sequence of actions, performing well at its assigned tasks while avoiding unexpected possibly harmful mistakes. This agent should also be trained with minimal supervision and hand-designed features, as these can be prohibitively expensive and may exceed our design abilities or understanding (Kormushev et al., 2013; Dulac-Arnold et al., 2019; Ibarz et al., 2021).

Training such an agent involves learning from *interaction data*, which is data drawn as the result of an embodied agent

performing actions on an environment, with reinforcement learning (RL, Sutton & Barto, 2018) and imitation learning (IL, Hussein et al., 2017) being well-studied classes of approaches. To capture interaction learning more generally, we define Learning from Interaction (LInt) as any setting where an agent is trained on interaction data to perform optimally on a set of sequential decision-making tasks, including offline / online RL, IL, Goal-Conditioned RL (GCRL, e.g., Schaul et al., 2015), Meta-RL (Gupta et al., 2018), etc.

Unfortunately, the added time and cost for training and evaluating agents (Berner et al., 2019), the inherent variability of (Kormushev et al., 2013; Zhu et al., 2020a), and potential catastrophic consequences in (Ibarz et al., 2021) real-world settings (see Ibarz et al., 2021, for a comprehensive discussion) can make LInt research directly in these domains prohibitively difficult. To aid in research, artificial environments have been created to make studying LInt more practical. Environments based on video games (Belle-mare et al., 2013; Cobbe et al., 2019) have demonstrated the usefulness of RL and IL algorithms to solve difficult tasks based on pixel-based observations (Schulman et al., 2017; Hessel et al., 2018). Environments that simulate real-world settings have improved our understanding of how LInt algorithms may be useful in domains such as robotic control (Zhu et al., 2020b; Ahmed et al., 2020) and autonomous driving (Dosovitskiy et al., 2017), and there are various promising approaches to transfer these successes to back to real-world settings (Zhu et al., 2018; Zhao et al., 2020).

While this progress is admirable, there has been less progress with agents that operate well under variation of tasks within an environment, an inevitable feature of real-world settings. The *task distribution* can describe variability of environment properties, such as the observation space, initial conditions, transition functions, or reward function. The task distribution can be related directly to variable criteria of “success” (e.g., variable return functions or initial conditions) or a distractor to success (e.g., noise in pixel-based observations). One can also expect in real-world settings that the agent will have a limited budget of training tasks, which can lead to overfitting thus poor performance at deployment, and the seriousness of this can depend on the complexity of the training and test task distributions (e.g., multimodality). The *objectives* we wish to highlight are those that involve

*Equal contribution ¹Most of the work done at Microsoft Research, Montreal ²Mila ³Currently at Apple Machine Learning Research ⁴McGill University ⁵Microsoft ⁶Microsoft Research. Correspondence to: R Devon Hjelm <devonh@apple.com>.

(A) Guide to good generalizable agent research

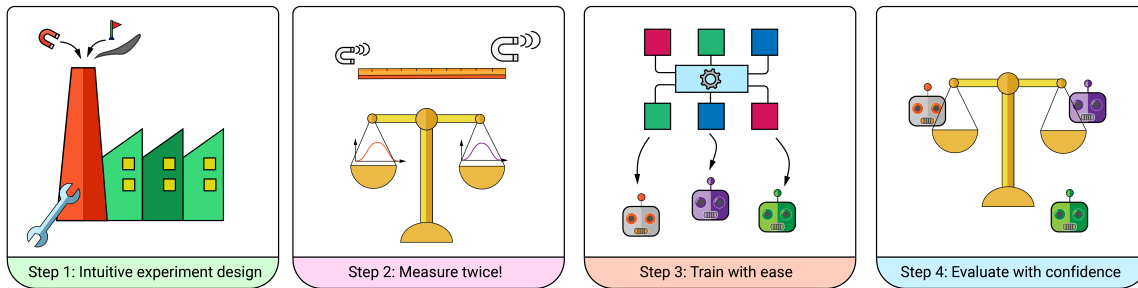


Figure 1. Our high-level motivation for designing SEGAR to improve generalization research in interactive settings, such as RL or IL. First, the researcher must have transparent, intuitive, and easy-to-use control over the experiment parameters. Next, the researcher must be able to use standard measures to evaluate their experiment design against others. Training a number of agents across algorithms and environment parameters should be easy, and the transparency and measurability on the environments should lead to more confidence in the conclusions of experiments.

good performance in different set of tasks at deployment than in training, in other words *generalization objectives*. Not evaluating agents on generalization objectives limits our ability to understand whether the agent learned spurious correlations between noise and signal (Song et al., 2019), truly understands the environment (Ke et al., 2021), can generalize from limited examples (Finn et al., 2016; Kahn et al., 2018), and can perform well in or adapt to tasks that are drawn out-of-distribution w.r.t. the training ones (Packer et al., 2018).

Thankfully, there has been a growing movement towards environments that facilitate progress towards this common objective (e.g., Packer et al., 2018; Cobbe et al., 2019; Song et al., 2019; Chevalier-Boisvert, 2021; Zhu et al., 2020b; Ahmed et al., 2020; Hafner, 2021, to name a few). Towards this goal, we developed the Sandbox Environment for Generalizable Agent Research (SEGAR), which we believe brings several crucial components into one place. SEGAR is designed from the ground up with generalization in mind by giving the researcher *intuitive and transparent control over task distributions*. In order to facilitate this, the underlying state space is fully exposed to the researcher with initial conditions fully specifiable by known parametric distributions. These features allow the researcher to implement *quantitative measures on experimentation*, such as those that measure how representative a set of training tasks are of their underlying distribution or how close a training task distribution is from the ones the agent is being evaluated on. This experimental measurability in turn improves accountability in experiment design. In addition, SEGAR is designed to be highly *customizable and easy to use*, allowing for extensibility on generalization experimentation. Finally, as we believe that studying the representation of interactive agents will be crucial towards developing better algorithms, we provide *means of evaluating representations*

of the agent w.r.t. the underlying state space. We note that, while we provide these built-in tasks and measures, SEGAR is designed from the ground up to be customizable and extensible in nearly any way, allowing the researcher to design new tasks with novel components and measures.

SEGAR can be found at <https://github.com/microsoft/segar>. Note that SEGAR is open-sourced under an MIT license, and some core features may change or be expanded on, so we suggest referencing the documentation found at <https://segar.readthedocs.io>.

2. Related Works and Motivation

It is standard to use a generalization objective to evaluate a supervised or unsupervised learning algorithm when the data is drawn i.i.d. Objectives can challenge a model’s ability to generalize in many ways, from succeeding despite limited training data (Tan & Le, 2019), to training on a few examples of some classes (e.g., few-shot learning (FSL) Wang et al., 2020), to correctly predicting classes not seen during training (e.g., zero-shot learning Xian et al., 2018), and to successfully adapt to distributional shifts (Zenke et al., 2017) without forgetting, to name a few prominent examples. Generalization objectives often are specified in terms of annotation, such as class labels, with different objectives “splitting” data samples into sets according to the annotations (e.g., a ZSL objective can be defined by through split that ensures that some annotations in the test set are not present during training). Annotation ultimately corresponds to some set of *factors of variation*, such properties of “entities”, such as a “cat” or a “fish”, for instance the presence of fur, ears, or fins, or other attributes such as shape, color, size, etc. While there is flexibility in how one “selects” and uses factors to design an objective, they are central to defining the generalization objective and understanding what success

implies to other problems.

In Learning from Interaction (LInt) settings, however, generalization objectives are less standard, though an increasing number of environments have emerged for this purpose (see Kirk et al., 2022, Section 4, for an extensive list). There is additional flexibility on whether the factors correspond to the states (e.g., static properties of the environment such as the score, not to be confused with things that do not change within an environment) or trajectories (e.g., the obstacles are moving to the right versus the left). For sake of simplicity, we treat the factors as *properties of entities in the environment*, separate from any dynamics due to the environment, the expert in IL settings, or the agent. In the remainder of this section, we will discuss some of the progress in defining generalization objectives for LInt settings and ultimately motivate the Sandbox Environment for Generalizable Agent Research (SEGAR).

2.1. Intuitive and transparent control over task distributions

Artificial environments provide a unique opportunity for LInt generalization objectives, as the complete set of underlying factors can be available for the researcher to use. Despite being an obvious advantage over human-annotated i.i.d. data settings, however, annotation is rarely used in interaction settings to specify generalization objectives. Usable annotation is completely absent from the Atari benchmark (Bellemare et al., 2013), though wrappers have been created to aid in representation learning research (e.g., Anand et al., 2019), which has meaning only within a single task “game”. Environments such as the Procgen benchmark (Cobbe et al., 2019) provide various degrees of control over procedural generation of the initial conditions (Chevalier-Boisvert, 2021), observation space (Fan et al., 2021), reward function (Küttler et al., 2020), action space (Zhu et al., 2020b), and combinations of these (Johnson et al., 2016; Hafner, 2021; Juliani et al., 2019), but the true distribution of the task may be obscured by a generative function made up of complex control flows.

A good LInt generalization benchmark should give researchers access to and control over task generation, yet be simple enough for a researcher to understand and intuitively predict how a given context’s combination of factors will translate to various properties of a task. For standalone discrete-state and -action tasks whose transition functions are expressible in terms of logical predicates, control over task generation is offered by description languages such as PDDL (McDermott et al., 1998) and RDDDL (Sanner, 2010) and tools such as PDDLgym (Silver & Chitnis, 2020) that compile task descriptions into simulators. For task *distributions*, various environments make advancements in this direction as well, such as CausalWorld (Ahmed et al., 2020),

MDP playground (Rajan et al., 2019), Textworld (Côté et al., 2018), and Mini-environments (Ke et al., 2021) which provide fine-grained and intuitive mechanisms that allow for controlling and varying the task parameters via distributions.

We designed SEGAR with this type of intuitive control and transparency in mind by making fine-grained control over the task distribution the starting point in our design. The initial values of all the underlying factors can be specified in terms of parametric distributions, and these factors directly control the initial state. In addition, the transition and reward functions are clearly defined in terms of these factors, meaning this distributional control extends to the rest of the task distribution as well.

2.2. Quantitative measures on experimentation

However, it is difficult to be confident in a generalization objective without quantitative measures that reveal the nature and hardness of generalization problems the objective represents, e.g., whether it be out-of-distribution, in-distribution sample efficiency, etc. Benchmarks with built-in measures on objectives are unfortunately rare outside of those directly related to parameters of task generation, such as those directly tied to the various dimensions that generate distributional shifts. MDP playground (Rajan et al., 2019) provides various measures that quantify the hardness of each task, and XLand (Team et al., 2021) provides an extensive set of metrics on trajectories / tile connectivity as well as resistance distance of single worlds, distances between worlds, diversity of worlds, etc.

As SEGAR starts from distributions, this allows the researcher to use a number of useful metrics across tasks, such as entropy and likelihood, as well as allow for quantifying how representative a set of samples are to their underlying distributions. These can be used to directly evaluate the objective, giving the researcher much-needed insight on the generalization problem it represents and into the ultimate research impact of a successful agent.

2.3. Customization and ease-of-use

Another crucial design choice of artificial environments is the structure and complexity of the underlying state space and transition functions, the choices of which can have significant impact on whether lessons learned in the environment apply readily to real-world settings as well as the cost of experimentation. A number of popular environments are video games (Bellemare et al., 2013; Cobbe et al., 2019; Team et al., 2021) or grid worlds (Ke et al., 2021; Chevalier-Boisvert, 2021) with visual observations and dynamics that have little relevance or resemblance to the real world. 3D video game environments (Team et al., 2021; Hafner, 2021; Johnson et al., 2016) include some more real-world physics (such as gravity), but the resemblances are overall small. A

number of robotic (Zhu et al., 2020b; Ahmed et al., 2020) and physics (Todorov et al., 2012) environments boast realistic physics with various degrees of customization, but always come with a large trade-off between speed, stability, and accuracy (Erez et al., 2015; Dulac-Arnold et al., 2019).

SEGAR strikes a balance between realism and cost through flexibility: allowing the researcher to easily structure the task in a way that reflects what they believe represents real-world settings, allowing them to pick and choose where to pay the cost of realism. We also believe that there is a substantial gap in all of the above features in 2D environments, as most of the environments that fulfill the above criteria are in 3D. Taking inspiration from Box2D (Catto, 2006), SEGAR fills this gap, with the goal of facilitating the movement from strong SOTA algorithms in 2D environments to more complex 3D ones (Kolve et al., 2017; Savva et al., 2019), where strong algorithms are in short supply. Finally, SEGAR is a sandbox environment, and as such provides a lot of experimentation flexibility: it allows for varying nearly every aspect of the environment, from the observation and state spaces to the dynamics and reward functions.

2.4. Representation evaluation

A widely studied class of approaches to building an agent or a model whose behavior generalizes to new circumstances is encouraging the agent to learn a latent *representation* of its inputs. The intent of learning such a representation is to encode information so as to retain only the content that is “useful” (e.g., translatable to downstream performance). In i.i.d. settings with no interaction, representations have received extensive study in term of the connection between intrinsic measures (Rigamonti et al., 2011; Gretton et al., 2012; Bengio et al., 2013; Kingma & Welling, 2013; Sylvain et al., 2019). Measures on intrinsic representational properties such as mutual information (Belghazi et al., 2018) and classification-based probes on ground truth annotation (Jaiswal et al., 2021), among others, can provide crucial insight into the success of models in downstream tasks.

There are a number of RL methods that use a representation learning loss function to improve performance an RL objective, whether related to generalization or not (Laskin et al., 2020; Mazoure et al., 2020; Schwarzer et al., 2020; 2021; Hafner et al., 2020; Mazoure et al., 2021; Yarats et al., 2021). However, despite the loss functions operating directly on the agent’s representation, the representations themselves are rarely evaluated beyond evaluating the returns, with some exceptions (Anand et al., 2019; Zhang et al., 2020; Mazoure et al., 2021; Lyle et al., 2021). Atari Zoo (Such et al., 2018) is one of a few comprehensive studies into the role of representations in downstream performance, and as

mentioned above: Atari is not a setting suitable for studying generalization.

However, if the underlying factors of the environment are known, it can be very straightforward to test what intrinsic properties of representations correspond to success on generalization objectives. As SEGAR provides fine-grained control over distributions of factors, we can intervene on these distributions and study the effect on the resulting representations as well as downstream performance. Finally, statically unobservable factors (e.g., mass oftentimes in real world settings), such as those found in partially-observable settings can perhaps be better understood in terms of the agent’s representations.

3. Terminology and setting definition

SEGAR is a sandbox environment and toolkit for defining generalization objectives via distributions of sequential decision-making *tasks*, automatically translating them to distributions of *partially observable Markov decision processes (POMDPs)*. SEGAR’s tasks have a special structure: they involve objects (*entities*) and *rules* that determine how the objects interact with each other depending on the objects’ latent properties (*factors*). The *metrics* that SEGAR is geared towards are meant to evaluate the nature of the generalization objective, as defined by the task distributions and their samples. In addition, we wish to evaluate how well different learners are able to infer tasks’ latent factors from the factors’ partially observable effects on object behavior, as reflected in the object interaction data available to the learner. In this section, we formalize all the highlighted terminology to set the stage for describing SEGAR’s tools in Section 4.

Task definitions are founded on the concept of **factor type**. Factor types are physical properties of objects, e.g., MASS, CHARGE, and POSITION. SEGAR provides a number of predefined factor types inspired by real-world physics and allows researchers to add new ones. We denote the set of all factor types available to a researcher as \mathcal{T}_{factor} .

Factor types give rise to the concept of **entity type**. Entity types are types of objects in SEGAR’s tasks, such as SAND or MAGNET. As with factor types, SEGAR provides several built-in entity types and lets the researcher add more. An entity type defines an ordered basis: $\mathcal{T}^e \triangleq (\mathcal{T}_{n_i}^f)_{i=1}^{N^e}$ over a vector space $\mathcal{X}_{\mathcal{T}^e}$, where the ordering is fixed by the environment, and the basis elements $\mathcal{T}_{n_i}^f \in \mathcal{T}_{factor}$ are factor types, each spanning a vector space, $\mathcal{F}(\mathcal{T}^e)_i$. The complete vector space of an entity type then is a product space $\mathcal{X}_{\mathcal{T}^e} = \prod_i \mathcal{F}(\mathcal{T}^e)_i$. The set of all available entity types is denoted as \mathcal{T}_{entity} .

Given these definitions, an **entity** in SEGAR is an instance of an entity type, i.e., a specific object, and a **factor** is an

instance of a factor type, i.e., a property of a specific object. E.g., if MASS, RADIUS, X, and Y are factor types and BALL = (MASS, RADIUS, X, Y) is an entity type, then $B_7 = (\text{MASS} : M_7, \text{RADIUS} : R_7, \text{X} : X_7, \text{Y} : Y_7)$ is a specific ball, and $M_7, R_7, X_7,$ and Y_7 are factors denoting B_7 's mass, radius, and position. Therefore, each entity of type \mathcal{T}^e is represented by a vector of factor values in $\mathcal{X}_{\mathcal{T}^e}$. Let \mathcal{E} be a finite multiset of entity types from $\mathcal{T}_{\text{entity}}$, e.g., {BALL, BALL, MAGNET, SAND, SAND}, where the element ordering is fixed by the environment. Then the complete space defined by \mathcal{E} is a product space, $\mathcal{X} = \prod_{\mathcal{T}^e \in \mathcal{E}} \mathcal{X}_{\mathcal{T}^e}$. The vectors $x \in \mathcal{X}$ have no special structure outside of the ordering of the entities and factors prescribed by the environment, so states can be interpreted as vectors on a product space over all factor spaces over all entities, $\mathcal{X} = \prod_{\mathcal{T}^e \in \mathcal{E}} \prod_i F(\mathcal{T}^e)_i$.

Entity interactions are governed by **rules**, \mathcal{R} . Let \mathcal{B} be the set of all multisets over entity types $\mathcal{T}^e \in \mathcal{T}_{\text{entity}}$. Note first that $\mathcal{E} \in \mathcal{B}$ from above, so like \mathcal{E} , every $b \in \mathcal{B}$ has a associated vector space \mathcal{X}_b over the multiset of entity types. For $b \in \mathcal{B}$, a rule, $r(b) : \mathcal{X}_b \mapsto \mathcal{X}_b$ is a function that applies to and modifies a vector of factor values over entities. Given a set of entities in the arena, applying the rule, $r(b)$, amounts to finding all combinations of entities with types that match b , then modifying their factor values as specified by the rule. There is additional logic to manage when multiple rules apply to the same entity's factor, and this is covered in Section 4.

The entity factors are observable through an **observation function** $z : \mathcal{P}(\mathcal{T}_{\text{factor}}) \times \mathcal{X} \mapsto \mathcal{O}$, where $\mathcal{P}(\mathcal{T}_{\text{factor}})$ is the power set over factor types. Values of factors dictating entity behavior may or may not be directly observable, as z is designed to only admit observations of a subset of all factor types. This indicates whether different values of a factor of a given type are manifested visually, e.g., as object color. z can be stochastically drawn from a larger set of observation functions.

The final components are the **action space**, \mathcal{A} , and the **reward function**, $r : \mathcal{X} \times \mathcal{X} \times \mathcal{A} \mapsto \mathbb{R}$. The action space is typically an input at an action function, $a : \mathcal{A} \times \mathcal{X} \mapsto \mathcal{X}$, which directly operates on the complete space over all entities.

Finally, we define a **task** in SEGAR, which is a tuple $\langle \mathcal{T}_{\text{factor}}, \mathcal{T}_{\text{entity}}, \{\mathcal{E}_{\mathcal{T}^e}\}_{\mathcal{T}^e \in \mathcal{T}_{\text{entity}}}, \mathcal{R}, \mathcal{A}, r, z, c_0 \rangle$, where c_0 is the initial configuration of all of the task's entities, i.e. an assignment of values to all entities' factors. For instance, if a task involves one ball and one charged ball, the initial configuration could be $c_0 = \{(\text{MASS} : M_1 = 3, \text{RADIUS} : R_1 = 0.2, \text{X} : X_1 = 5.32, \text{Y} : Y_1 = 1.04), (\text{MASS} : CM_1 = 3, \text{RADIUS} : CR_1 = 0.2, \text{X} : CX_1 = 2.11, \text{Y} : CY_1 = 6.97, \text{CHARGE} : CC_1 = -10)\}$.

SEGAR'S major contribution are tools for imperatively defining **task distributions**. Sampling a task entails first constructing \mathcal{E} by generating a number of entities of each type. Then, the initial configuration, c_0 is drawn by sampling an initial value for every factor of every generated entity from a set of given priors.

SEGAR compiles every task into a mathematical formalism widely adopted in IL and RL, a **POMDP**. For a task T , POMDP M_T is a tuple $\langle \mathcal{X}, \mathcal{A}, T, r, \mathcal{O}, z, x_0 \rangle$, where the state space \mathcal{X} , the action space, \mathcal{A} , the reward, r , the observation function, z are defined as above, \mathcal{O} is the observation space induced by z , and $P : \mathcal{X} \times \mathcal{A} \mapsto \Delta(\mathcal{X})$ is a transition function induced by T 's rule set \mathcal{R} . The mechanisms for combining rules into a transition function will be covered in Section 4. Finally, x_0 is the POMDP's initial state, derived from the factor values from T 's initial configuration c_0 . Depending on the optimization objective, an optimal POMDP solution is a **policy** $\pi : \mathcal{H} \mapsto \Delta(\mathcal{A})$ that maps histories of observations $h_t \in \mathcal{H}, h_t = o_t, o_{t-1}, \dots, o_1$ to action distributions.

4. The Sandbox Environment for Generalizable Agent Research

This section provides an overview on how SEGAR is structured as a programming interface for the goal of designing generalization objectives for LInt generalization research. SEGAR is functionally split two parts: an environment and a set of experimentation and representation *metrics*. The environment is composed of:

- A *state space*, \mathcal{X} , which is composed of all factor type vectors of the entities in the task. The state space is only determined after the numbers and types of entities have been sampled by the environment for the task.
- A **SIMULATOR**, which organizes the entities, factors, and rules, and ultimately implements the *transition function*, P .

The environment generates tasks, T , which in turn compiles into a MDP object. The MDP class has the following class members:

- An **OBSERVATION** object, which defines the function, z , between states and observations, as well as which factors are observable. This could also include a renderer for pixel-based observations, which operates as a function between states and visual features.
- A **TASK** object, which is composed of:
 - An **INITIALIZATION** object, which determines the initial state, s_0 , by sampling the number of

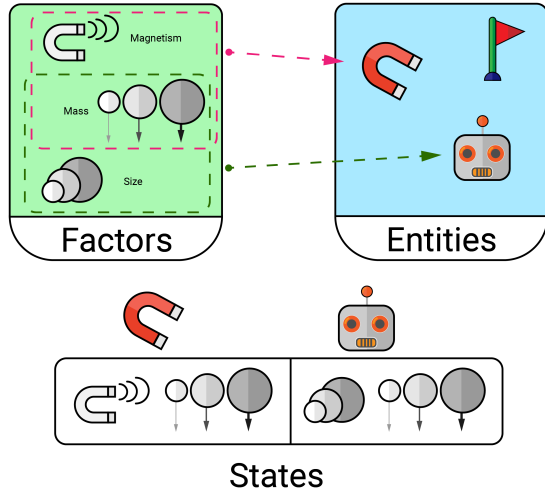


Figure 2. An example state space from SEGAR. This state space is a product of two vector spaces, each corresponding to an entity. Each entity contains a different set of factor types, which make up the basis of each entity vector space. The complete state space is not structured beyond being a vector space and the basis ordering fixed by the environment. Note that the state space in SEGAR can be of arbitrary size, depending on the numbers and types of entities in the task.

and type of entities, \mathcal{E} , as well as their initial configurations, c_0 .

- An *action space*, \mathcal{A} , which determines how the agent can directly change the underlying states.
- A *reward function*, r , which defines the returns.

All of these components are encapsulated in an MDP object, as illustrated in Figure 8, which is implemented as a OpenAI Gym environment (Brockman et al., 2016). This makes SEGAR easily usable with existing LInt algorithms that already build off of Gym. In the next sections, we will present the above components of the environment and describe how each can be used to aid in generalization experiments.

4.1. State space

An overview of the state space is provided in Figure 2. The SEGAR states are composed of a set of *entities*, and the entities are composed of a set of *factors*. For each task, the INITIALIZATION object (see below) samples the number of a given set of entity types, \mathcal{T}_{entity} , resulting in a finite multiset of entity types.

Each entity type, \mathcal{T}^e , has a unique set of factor types, $\mathcal{T}_{factor}^e \subseteq \mathcal{T}_{factor}$. Some examples of the factor types include:

- **POSITION:** A 2D vector representing the location of an entity within the arena.

- **CHARGE:** The charge of the entity, used to determine dynamics from the Lorentz law of electromagnetic force (Panofsky & Phillips, 2005).
- **MASS:** Inversely proportional to how much force needs to be applied to change the velocity of an entity.
- **FRICTION:** The kinetic friction coefficient of a TILE used to compute the force due to friction applied to another entity (such as an OBJECT).

A complete list of SEGAR’s built-in factors can be found in the documentation. Note that the set of factor types \mathcal{T}_{factor} is extensible through sub-classing any existing factor type (including the generic FACTOR type).

The set of entity types, \mathcal{T}_{entity} are all sub-classes of the ENTITY generic class, and their factor types are implemented as a set of dictionary keys. For example, the dictionary representation for an entity might look like:

```
{
  Position: [0.1, -0.1],
  Mass: 0.4,
  Velocity: [0.1, 1.0],
  Shape: Circle,
  ...
}
```

Like factors, the set of entity types, \mathcal{T}_{entity} , can be expanded by sub-classing. Some examples of built-in entity types include:

- **ENTITY:** Abstract container of factors. Can be thought of as a dictionary with factor types as key entries and the corresponding factor values as the values.
- **THING:** An entity with position, shape, and size factors. These correspond to the class of entities that are “localizable” in the arena, i.e., through their position, location, and shape.
- **OBJECT:** A thing that has mass, charge, and other object-like factors, but most importantly have velocity. Objects move around in the arena and collide with walls and other objects.
- **TILE:** A thing that does not move nor collide, but can apply force to objects that overlap with them. Tiles can also have friction or heat, the latter of which changes the mass of objects that are on top of the tile.

We provide a full list of built-in entity types in the [documentation](#).

4.2. Simulator, rules, and the transition function

An overview of the rules and how they are composed for the transition function are provided in Figure 3 and Figure 4. The SIMULATOR is the “brain” of the environment:

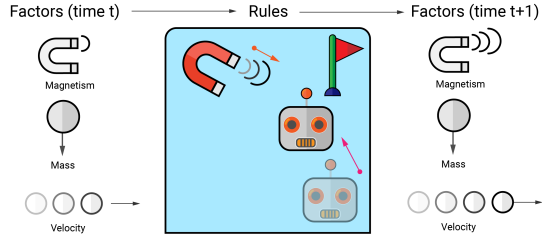


Figure 3. An example rule in SEGAR. This rule involves three factors: mass, velocity (through acceleration), and magnetism. The SEGAR simulator finds entities with the appropriate factors and uses the matching rules to change those factors, simulating a transition in state.

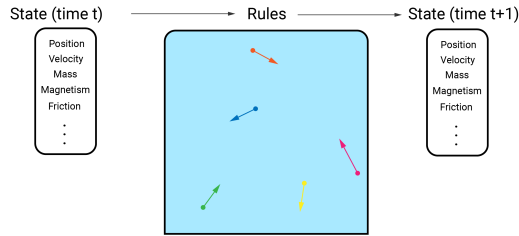


Figure 4. The transition function is computed by the simulator, which applies the appropriate rules to the appropriate factors. It does so by finding the entities that “match” the set of given rules, resolves conflicts when more than one rule applies to the same factor of the same entity, and manages collisions after positions change.

it organizes the rules, entities, and factors, finds, applies the appropriate set of rules to each entity, and manages collisions. The collection of rule applications along with collision dynamics make up the overall *transition function*, P , of the POMDP.

SEGAR allows the user to specify the set of rules, and the simulator applies those rules to all of the entities active in the arena of the task. Which entities apply to which rule is determined by pattern matching using the Python type hints system (see <https://docs.python.org/3/library/typing.html>). For example, the following rule applies friction on one entity from another entity (see Figure 3 for an illustration of another example):

```
def apply_friction(
    o1_factors: Tuple[Mass, Velocity, Acceleration],
    o2_factors: Tuple[Friction],
    gravity: Gravity) -> Aggregate[Acceleration]:
    mass, velocity, acceleration = o1_factors
    mu, = o2_factors
    if velocity.norm() >= 1e-6: # Ignore if velocity is small

        vel_sign = velocity.sign()
        vel_norm = velocity.norm()

        f_mag = mu * gravity
        norm_abs_vel = velocity.abs() / vel_norm
        da = -vel_sign * f_mag * norm_abs_vel / mass
        return Aggregate[Acceleration](acceleration, da)
```

This rule takes as input two tuples, one with mass, velocity, and acceleration, and the other with friction. This tells the simulator to search for all pairs of entities that contain *at least* these sets of factors, then marks these pairs as being valid input for this rule. As such, if a rule applies to an entity type, \mathcal{T}^e with factor types \mathcal{F}_{factor}^e , it will apply to a sub-class of \mathcal{T}^e , $\mathcal{T}^{e'}$ with factor types $\mathcal{F}_{factor}^{e'} \supseteq \mathcal{F}_{factor}^e$.

In order to handle multiple rules applying to potentially the same entity’s factors, we implemented a simple logic managed by the simulator to decide what rules to apply (resolve rule conflicts) and how (if at all) their results combine. The output of the above rule, for example, is typed to *aggregate* the change in the acceleration factor, so that the result of this rule should be added with any other rules that aggregates the same factor.

Overall, there are three output types in SEGAR:

- **AGGREGATE:** All rules that apply to the same factor and that have this type should be added, forgetting the previous value.
- **DIFFERENTIAL:** The result of this rule should be added to the prior value of the factor, scaled by the time-scale of the task.
- **SETFACTOR:** This overrides all other rule types and sets the factor directly to the output value.

For conflict resolution, SETFACTOR will override all other rule types, and AGGREGATE will override DIFFERENTIAL. If there is more than one SETFACTOR applied to the same factor, then there is additional logic based on how specific the rule is (e.g., is it conditioned on other factors of the same entity). If the logic ultimately can not resolve a rule conflict, then this will result in an error. There are also a set of special rules, collisions, which are always applied last after position factors have changed. SEGAR provides a set of built-in rules, the details of which are provided in the [documentation](#). However, like the factor and entity types above, the build-in rules are optional and extensible: the researcher may provide any set of rules they would like to the simulator, as long as they follow the same type hints system as the built-in ones.

4.3. Observations and Renderings

SEGAR allows the user to chose how the agent sees the underlying states, and an overview of the observation function is provided in Figure 5. The user may also specify any number of factors to include or omit from the observation space, allowing full flexibility in defining an MDP, POMDP, or block MDP.

The *observations* in SEGAR are implemented as a callable OBSERVATION object, which are passed to the MDP object

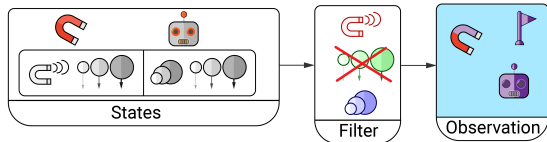


Figure 5. The observation function in SEGAR can be customized by the researcher as any function of the input states. Addition functionality for filtering factors given a type of observation function (such as state- or pixel-based) gives additional control over whether the problem is a MDP or a POMDP with respect to specific factors.

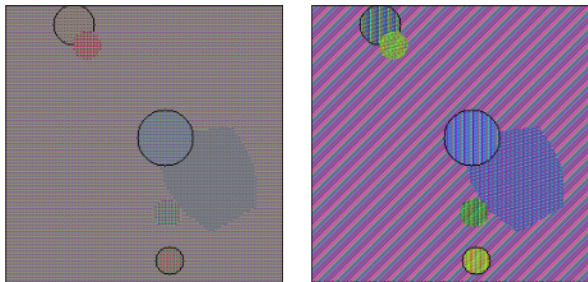


Figure 6. Two example visual renderings of the state state from SEGAR. Colors and patterns correspond to different factors and their values, with one pattern corresponding to the background. Left) Visual features from a trained auto-encoder where the input is drawn from the product of marginal uniform distributions over all factors. The agent should be nearly guaranteed to be able to infer all factor values from visual features. Right) Visual features derived from clustering the weights from the first layer of an Inception network.

for training the agent. Built-in classes include full state-based observations (all entities), partial state-based observations (some of the entities), 2D pixel-based observations, and multi-modal observations built from any combination of these, and observations are extensible through sub-classing.

For the pixel-based observations, SEGAR provides built-in *renderers* that generate visual features from the underlying factors. Two examples are provided in Figure 6. The first built-in renderer is trained from scratch using an autoencoder, with an encoder that takes samples from the marginal distribution over factor types as input and outputs visual features in RGB pixel space. The autoencoder is given a reconstruction network and the full model is trained to reconstruct samples from the product of marginals. The second built-in renderer is constructed from the first layer weights from an Inception network trained on Imagenet (Szegedy et al., 2017) along with a k-means to cluster these weights, randomly associating each cluster with a factor type. We provide sets of both of these renderers, generated with different initial seeds, allowing for measurable variation across observation spaces (see Figure 7 for examples of the auto-encoder renderer given the same state).

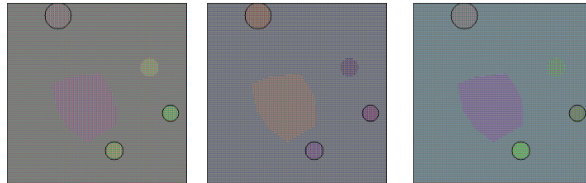


Figure 7. Provided variants of linear auto-encoder visual features allows the user to vary the observation space, challenging the agent’s ability to adapt to environments with the same physics, yet different visual features. These are generated from different auto-encoders trained with different seeds. Similar variants are provided for the the Inception renderer.

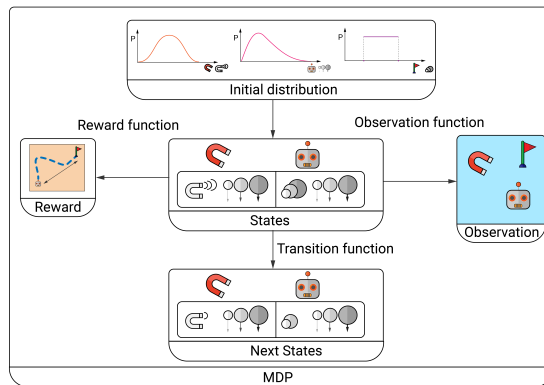


Figure 8. The complete MDP generated for a task. Distributions are used to sample the task, which selects the initial states of the environment, and the researcher can specify the reward function and observation space for the agent. A Transition function is by a simulator with customizable rules.

Though we provide a built-in renderer for researchers to use, we believe that providing observations to the agent based on visual features that are understandable by humans may unintentionally introduce experimental challenges, as neural networks can leverage low-level visual cues to “cheat” at tasks that were intended to require higher-level reasoning. In SEGAR, the visual features are treated as a transparent and controllable component in building experiments, such that the research can control how the underlying factors are expresses in terms of pixels, if at all. In addition, we allow for researchers to design their own observation spaces and renderers to better reflect the domain they wish to study.

4.4. The Task

The final component in SEGAR is the TASK, which encapsulates the INITIALIZATION object, the reward function, and the action space, as well as points to the SIMULATOR and OBSERVATION objects. SEGAR comes with three built-in demonstration tasks: PUTTPUTT, BILLIARDS, and INVISI-BALL, though SEGAR was designed to easily allow users

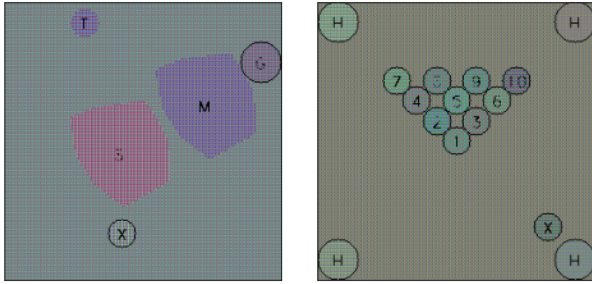


Figure 9. The visual renderings of two example built-in tasks from SEGAR. Left: Putt-Putt, the agent can apply force to the ball (“X”) and gets reward if it reaches to goal (“G”). “M” is magma, which reduces the ball’s mass, “S” is sand which applies friction. “T” is a magnet, which accelerates the ball according to Lorentz law. Right) Billiards: the agent has control over the cueball (“X”) and must get the balls (numbered 1 to 10) into the holes (“H”). Note: the text annotations are for human-readability only and are not provided to the agent.

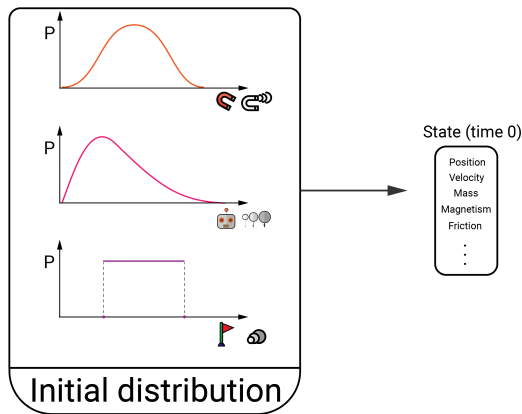


Figure 10. SEGAR allows for specification of the distribution from which tasks are drawn, in the above case in terms of initializations.

to define new tasks within the framework.

- **PUTTPUTT:** Navigate a ball around various obstacles to a goal location.
- **BILLIARDS:** Controlling a cueball, use collisions to knock the other balls into holes.
- **INVISIBALL:** PuttPutt, but the ball is invisible after the first step. The ball has charge and there are other objects that also have charge, so the agent needs to infer charge and position of the other objects through the movement of the other objects.

In addition, SEGAR allows defining training and test task distributions for generalization experiments. Such experiments are a major motivation behind SEGAR’s design, and

SEGAR makes them easy to set up by specifying distributions over generative factors’ values for training and test tasks.

Initialization The `INITIALIZATION` object controls which entity types are initialized and what their initial factor values are, ultimately sampling the initial state, s_0 . The `INITIALIZATION` object allows for specification of the initial entity configuration, c_0 through distributions, and different initial conditions can be sampled to generate multiple tasks from the same `INITIALIZATION` object. The parameters of these distributions are specified through a `PRIOR`, which is a special type of rule that samples factor values from given parametric distributions. This allows researchers to specify their tasks through known parametric distributions (such as Gaussian, Uniform, etc).

Reward function Reward functions defines what success means for the agent in an environment, and SEGAR allows an experiment designer to easily construct them from the underlying states and the the agent’s actions. The reward function is implemented as a simple Python function that takes the states and actions as input and outputs a scalar.

Action space The action space is the combination of a Gym space and a function which operates directly on the factors of the environment. For example, a “force” action on a ball would change the velocity factor of the ball instantaneously. Valid actions are determined by a function that interacts directly with the entity factors through the simulator, so a designer is not limited on what factors the agent can intervene on through its actions.

4.5. Metrics on experimentation and representations

The second part of SEGAR are metrics, both on objectives and representations. The former is in place to add accountability to design: without metrics on LInt tasks it is difficult to assert that generalization “success” could – or even should – imply success in other settings, notably real-world ones. This is made possible as SEGAR allows the researcher to define the MDP in terms of distributions. In addition to providing control over and access to these distributions, SEGAR provides access to statistics on these distributions, such as CDFs, PDFs, entropy, etc (see Figure 11). Using these statistics, we can easy derive the entropy of the initialization, as well as measure how similar two distributions of initialization are. In addition, we can measure how representative a set of samples, say a training set, are to the underlying distribution they come from using statistics such as the Kolmogorov–Smirnov test (Smirnov, 1948), or even from training samples to the test distribution. Finally, we can use the Wasserstein-2 distance (Rüschendorf, 1985; Flamary et al., 2021) to compute distances between sets of tasks (say

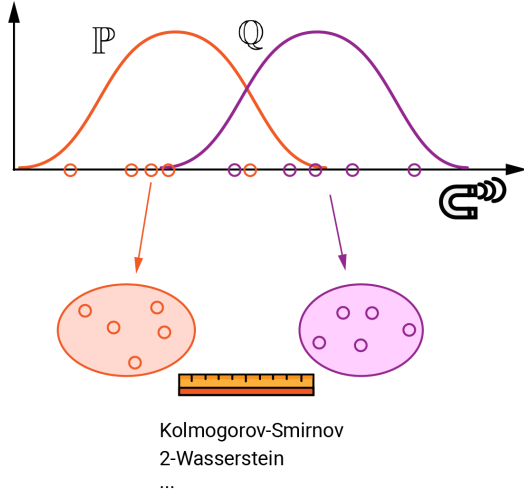


Figure 11. As the underlying factors are exposed and their underlying distributions known, there are many ways to measure the distance between sets of tasks as well as between sets of tasks and task distributions. This includes Kolmogorov-Smirnov (sample to distribution) and Wasserstein-2 (sample to sample) distances.

train vs test) through their initializations. Note that there are a number of proposed ways to measure distances between MDPs (Agarwal et al., 2021), and as SEGAR provides full exposure to the underlying factors and their distributions, we look forward to their further development and inclusion.

For representation evaluation, we have full access to the underlying state space, so we can use mutual information as a measure for the agent’s understanding of the state space. We use Mutual Information Neural Estimation (MINE, Belghazi et al., 2018) but use a less biased version based on the Jensen-Shannon divergence (Hjelm et al., 2018; Poole et al., 2019). As this amounts to training a classifier, we can provide accuracy as a score for how well the agent understands the underlying factors. These metrics are explored in the following sections as examples of analysis possible using SEGAR.

5. Experiments

SEGAR was designed to facilitate generalization research in Learning from Interaction (LInt) settings. In this section we demonstrate some of the experiments possible using SEGAR that show that having a way to create distributions of train / test splits along with being able to measure various properties of the task distributions or agent representations can lead to insightful results.

SEGAR is primarily a tool which can answer important questions regarding generalization of learning agents and their world representations. Some of these questions include, “How does the performance of an agent trained on task

set A and tested on task set B correlate with the distance between sets A and B?” and “Does an agent need to properly identify the various latent factors of an environment such as position, velocity, mass and gravity for better generalization performance?”. We attempt to provide an answer these questions in a controlled experimental setup, defined below.

Experimental setup. Let \mathbb{P}_{train} and \mathbb{P}_{test} two task distributions on the same support. Since, in practice, their distribution functions are unknown, the learner has only access to sample tasks $T_1, \dots, T_n \sim \mathbb{P}_{train}$ and $T'_1, \dots, T'_n \sim \mathbb{P}_{test}$, and their corresponding sets of parameters. We first form an episodic POMDP (Ghosh et al., 2021) out of T_1, \dots, T_n , where every episode is samples from one of the n tasks uniformly at random. We then fit a PPO agent (Schulman et al., 2017) on this new environment, and train it until convergence of returns, or exactly 1M environment steps. After that, the agent’s policy and value networks are snapshotted, and can be re-used in all representation learning probes described later in this section. In addition, we include Pearson’s ρ correlation and the corresponding p -value for plots where linear trendlines are fitted. For all plots, we treated points with a standard score of 3 or greater as outliers and removed them from our analysis.

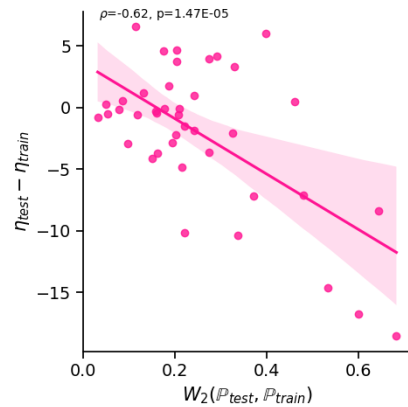


Figure 12. Generalization performance gap of a PPO agent as a function of the Wasserstein-2 distance between samples of the training and test distributions. Each dot represents an experiment on a different environment.

Does factor distance correlate with generalization gap?

How does an agent trained only on experiences from T_1, \dots, T_n re-uses this knowledge to solve T'_1, \dots, T'_n ? Intuitively, the more \mathbb{P}_{train} and \mathbb{P}_{test} overlap, the more information about one can be used to solve the other. We tested this hypothesis by jointly training an agent on T_1, \dots, T_n , and subsequently measuring it’s average performance η_{train} on \mathbb{P}_{train} and η_{test} on \mathbb{P}_{test} via independent rollouts. Then, the pairwise Wasserstein-2 distance between two tasks T_1, T_2

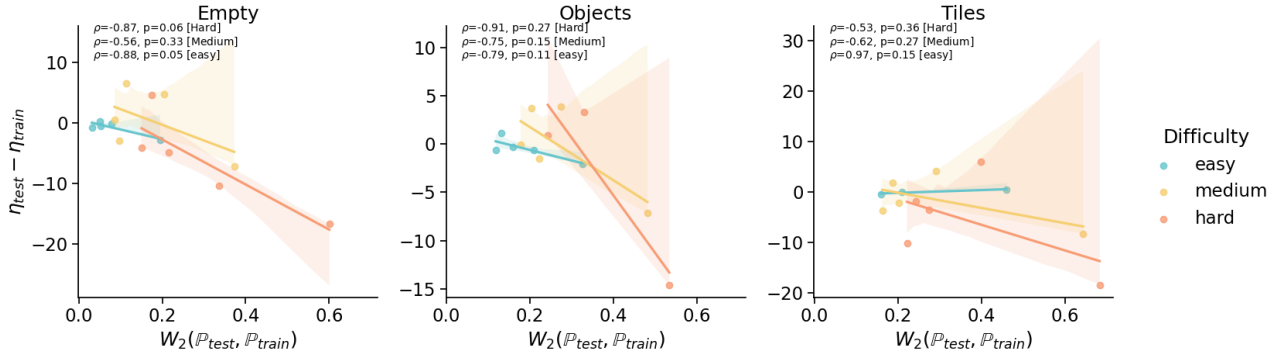


Figure 13. Generalization performance gap of a PPO agent as a function of the 2-Wasserstein distance between samples of the training and test distribution, split by environment type and difficulty. Each dot represents an experiment on a different number of levels and $\mathbb{P}_{train} \stackrel{d}{=} \mathbb{P}_{test}$.

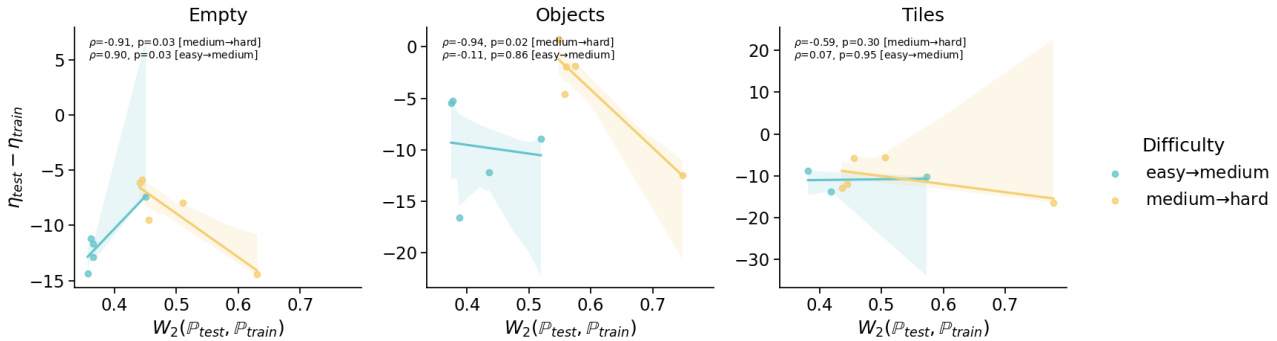


Figure 14. Generalization performance gap of a PPO agent as a function of the 2-Wasserstein distance between samples of the training and test distribution, split by environment type and difficulty. Each dot represents an experiment on a different number of levels. The test distribution was formed by increasing by one the difficulty (read entropy) of the training tasks (easy to medium, medium to hard).

can be computed by solving the classical optimal transport problem with a Euclidean cost between factor values. Both the performance and Wasserstein gaps are shown in Figure 12, which indeed shows a significant correlation ($p = 1.47 \times 10^{-5}$) between better performance on unseen tasks and similarity of these tasks to the training samples.

Additionally, Figure 13 breaks down the effects between various environment types: those with only agent and the goal entities, those with objects (such as magnets) and with tiles (such as sand), as well as by difficulty levels. The difficulty levels are regulated by the entropy of the task distribution \mathbb{P}_{train} . The trend of the generalization gap clearly worsens for all tasks as the Wasserstein-2 distance increases, with exception to the easiest tasks, where there is no clear trend. However, this trend is not as clear beyond the “Empty” level, as “Objects” and “Tiles” levels are weakly significant at best.

Finally, Figure 14 shows the decrease in performance which happens when transferring a pre-trained agent onto a harder set of tasks (easy→medium and medium→hard, respectively). In this setting, the performance gap is considerably larger than the one in Figure 13, since the distribution of test tasks is harder. Similar to previous results, there is a trend for the generalization gap to worsen with larger distance between train and test increasing for medium→hard, at least with “Empty” and “Objects”, but no clear trend for easy→medium.

Does mutual information between state representations and factors correlate with generalization gap? So far, we’ve identified some correlations between the generalization gap and factor distance between tasks. Yet, nothing was stated about the internal world representation that the agent adopts from task samples T_1, \dots, T_n . We conducted a second set of experiments to probe the state representation

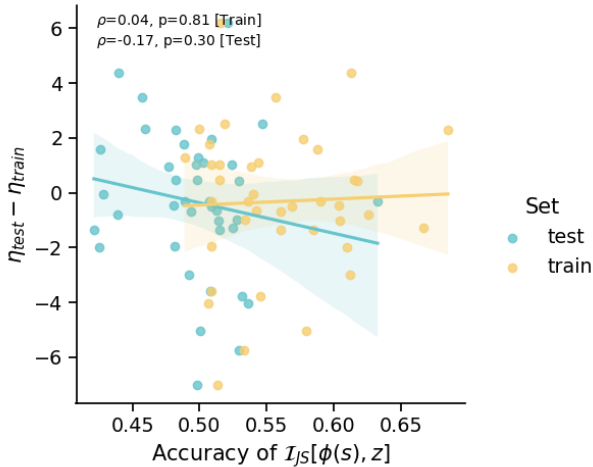


Figure 15. Generalization performance gap of a PPO agent as a function of the lower-bound on mutual information between learned state representations and environment factors. Each dot represents an experiment on a different number of training levels.

that an agent has about \mathbb{P}_{train} and \mathbb{P}_{test} by only having access to T_1, \dots, T_n . To do so, we first trained a PPO agent on T_1, \dots, T_n until convergence. The trained encoder was then used to map pixel observations onto latent representation vectors. We then used the MINE estimator (Belghazi et al., 2018) parameterized by a simple two-layer MLP to measure the lower-bound on mutual information between these latent representations and the entire set of factors associated with that observation; we denote this lower-bound based on the Jensen-Shanon divergence as $\mathbb{E}_{s,z \sim \mathbb{P}^\pi} [\mathcal{I}_{JS}(\phi(s), z)]$, as outlined in Poole et al. (2019). Rather than reporting the mutual information, which is unbounded, we report the classification accuracy of the MINE estimator on the binary decision task, which is bounded between 0 and 1.

Figure 15 shows the performance of an RL agent as a function of the lower-bound on mutual information between learned state representations and environment factors. We train on an increasing number of task samples, while testing on 500 tasks from the corresponding training distribution. While the train tasks score higher than the test, there is no relationship between performance and our mutual information estimates, at least with PPO.

What happens when we omit critical factor information (e.g. mass) from observations? So far, the tasks-specific factors have been fully observable through the feature mapping in the image embeddings of each entity. However, this scenario is highly unrealistic - it is rare that we can directly observe mass, friction, gravity, elasticity of real-world objects. More often than not, a handful of the factors can

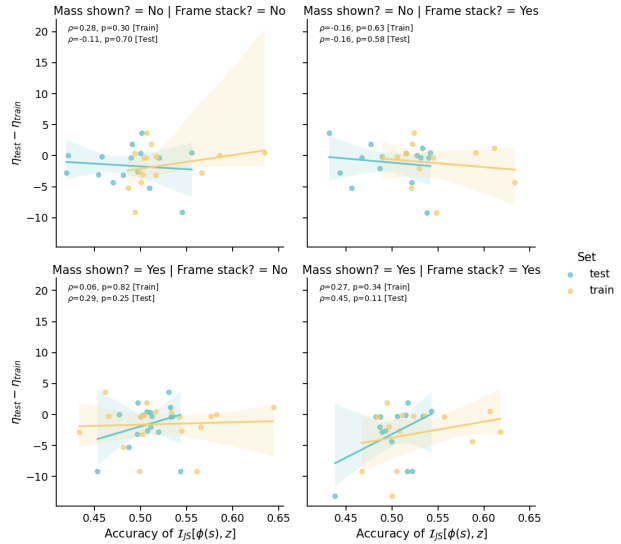


Figure 16. Generalization performance gap of a PPO agent as a function of the accuracy derived from the mutual information between learned state representations and environment factors, when including/ hiding the mass values, as well as adding/removing frame stacking. Each dot represents an experiment on a different number of training levels.

be sensed directly, while the rest is hidden and has to be extracted from observations. We simulated such a setup in the following experiment, where the mass factor for all entities was removed from the feature maps, making the task specification partially observable. One way to remedy to this issue is, at least in theory, to let the agent observe a sequence of observations via frame stacking. This lets the agent keep track of a "belief state" which can allow the agent to figure out the missing latent factor values based on the dynamics summarized in those observations.

Figure 16 show the results of this experiment. In particular, note how knowing the mass flips the performance gap trends (within the same task distribution), and helps achieve lower gap value for higher mutual information accuracies.

Do self-supervised representation learning objectives help extract factor information? In the past years, unsupervised and self-supervised representation learning methods have been empirically shown to significantly improve generalization capabilities of classical RL agents (Laskin et al., 2020; Mazoure et al., 2020; Schwarzer et al., 2020; Mazoure et al., 2021). But do these popular representation learning methods improve the understanding of the RL agent of the underlying latent factors?

Figure 17 shows the generalization performance gap as a function of accuracy derived from the mutual informa-

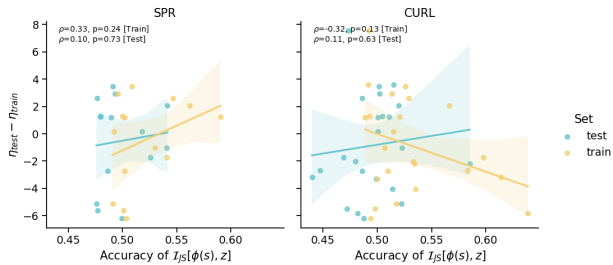


Figure 17. Generalization performance gap of a PPO agent as a function of the accuracy derived from the mutual information between learned state representations and environment factors, when adding predictive and contrastive self-supervised objectives. Each dot represents an experiment on a different number of training levels.

tion between states and factors for two such popular self-supervised learning(SSL) methods, CURL (Laskin et al., 2020) and SPR (Schwarzer et al., 2020). SPR, which relies on predicting exponentially-averaged copies of previous representations, appears to obtain a better generalization gap with higher information content, but only at training. Evaluation performance appears to be similar for both SSL methods as compared to vanilla PPO. However, as both SPR and CURL rely on data augmentations, it could be that the augmentations used for the original baselines they were evaluated are ill-suited for other observation spaces. Finally, as the JSD-based mutual information estimator is high variance (Poole et al., 2019), none of the apparent trends are significant, so either more samples or a lower-estimate estimator should be used.

Does the RL agent learn well-performing policies? Finally, Figure 18 shows the learning performance of various PPO agents as a function of training samples, on different environments, difficulty levels and number of task samples. We can see that the learning is fairly sample-efficient for easier configurations of the tasks, while harder tasks (e.g. with wider variations, objects and tiles) require the agent to train on much more samples before seeing reasonable performance.

6. Discussion

The Sandbox Environment for Generalizable Agent Research (SEGAR) is an open source sandbox environment designed for generalization research in settings with interaction data, e.g., Learning from Interaction (LInt). We demonstrated some of ways we envisioned SEGAR could be used, but due to limited time and resources we were not able to demonstrate nor test everything we had in mind and implemented.

Optimal policies and expanding task distribution configurations and benchmarks We selected only a few possible configurations of distributions of tasks, labeling them according to the known properties of distributions, such as entropy, and the numbers of and types of objects in the scene. We limited these configurations based on the performance of PPO, which due to time and compute constraints is the main RL algorithm we explored. A number of other baselines exist that could solve tasks within SEGAR much better than PPO (e.g., Hafner et al., 2020), and testing these stronger baselines could substantially change the picture as far as what is solvable under SEGAR’s full configuration capabilities. This, in turn, would lead to a larger set of more interesting generalization objective benchmarks.

Additional measurements on distributions and sets of tasks Among these included measuring properties of sets of tasks, such as entropy or variance, and comparing this measure to performance on the generalization objective. It would also be interesting to study how specific diversity measures on train and test tasks would reveal important information on the hardness of the generalization objective those task represent.

Quantitative measure of hardness based on the reward The reward function in SEGAR is flexible and can be clearly related to the underlying factors. For example, a PuttPutt task could be made more complex by conditioning the reward on more factors or events, such as only giving reward for reaching the goal only after it has also “rolled” over sand, or require one or more collisions in the process of reaching the goal. A researcher could use intuitive reward design to scale the hardness, measuring how different algorithms respond to this scaling.

More comprehensive measures on tasks and MDPs Measuring tasks based on the initial state or the distribution those states were drawn from are admittedly a small part of the full task, as the full task involves the dynamics due to the transition function as well as the reward. A key difficulty is that task diversity in terms of dynamics is entangled with the agent’s policy, though there are measures between sets of task assuming the optimal policy (Agarwal et al., 2021) that are relevant in transfer learning settings. Other measures that could separate the exogenous versus endogenous components of the MDP (Dietterich et al., 2018) to possibly measure how controllable a set of tasks are as well as use the uncontrollable components to build a policy-agnostic measures. These sorts of measures could provide a more comprehensive look of how a set of tasks vary or how different two sets of tasks are.

Varying rules of the environment SEGAR is fully capable of providing generalization objectives that involve

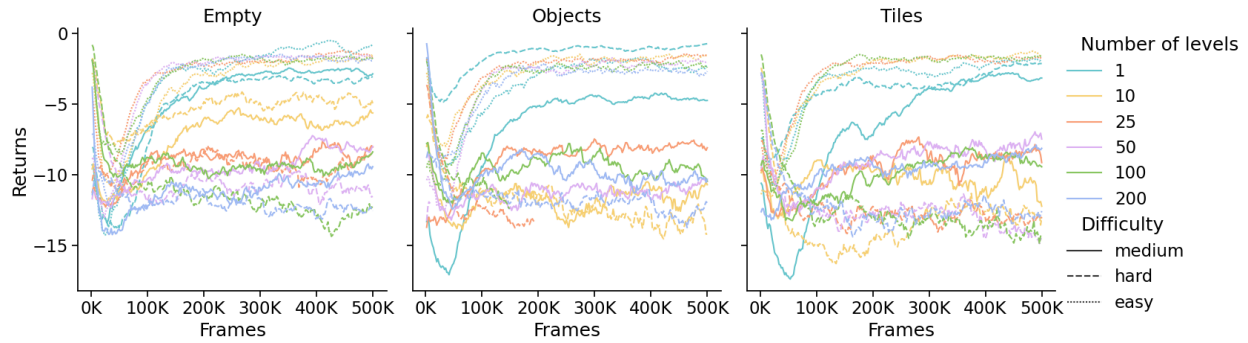


Figure 18. Performance of a PPO agent as a function of training frames. Each curves represents a different task, difficulty and number of levels configuration.

when the rules change, as this can be done by conditioning the rules on abstract entities whose role is only to provide abstract variable factors that modify those rules, such as the gravitational constant. One interesting direction would be to explore how variation in the rules effect performance of standard baselines, as well as how agents respond to distributional shifts.

Relationship between visual variation and performance

The generative models for rendering visual features of pixel-based observation spaces are simple with easy-to-access parameters. That said, we should be able to gauge how different one generator is from another through those parameters, as well as how different sets are. This control induces a number of experiments similar to those in the previous section, except involving the observation space.

There are a number of other applications that would demonstrate SEGAR’s potential impact to the LInt community as a whole. In addition to this, SEGAR could be used to develop video benchmarking data as well, potentially making it useful for video comprehension research. If the reader wishes to discuss their own generalization objectives or related analyses, please feel free to reach out via the GitHub issues.

7. Acknowledgements

We would like to thank Microsoft Research (MSR) for their generous grant to help support this research, fostering collaboration between MSR and Mila: the Quebec AI Institute. We would also like to thank Mila for their ongoing support and strong research culture, without which this research would not have been possible. Finally, R Devon Hjelm would like to thank MSR for their strong research culture as well as Apple MLR for allowing him to complete this work.

References

- Agarwal, R., Machado, M. C., Castro, P. S., and Bellemare, M. G. Contrastive behavioral similarity embeddings for generalization in reinforcement learning. *arXiv preprint arXiv:2101.05265*, 2021.
- Ahmed, O., Träuble, F., Goyal, A., Neitz, A., Bengio, Y., Schölkopf, B., Wüthrich, M., and Bauer, S. Causalworld: A robotic manipulation benchmark for causal structure and transfer learning. *arXiv preprint arXiv:2010.04296*, 2020.
- Anand, A., Racah, E., Ozair, S., Bengio, Y., Côté, M.-A., and Hjelm, R. D. Unsupervised state representation learning in atari. *Advances in Neural Information Processing Systems*, 32, 2019.
- Belghazi, M. I., Baratin, A., Rajeshwar, S., Ozair, S., Bengio, Y., Courville, A., and Hjelm, D. Mutual information neural estimation. In *International conference on machine learning*, pp. 531–540. PMLR, 2018.
- Bellemare, M. G., Naddaf, Y., Veness, J., and Bowling, M. The arcade learning environment: An evaluation platform for general agents. *Journal of Artificial Intelligence Research*, 47:253–279, 2013.
- Bengio, Y., Courville, A., and Vincent, P. Representation learning: A review and new perspectives. *IEEE transactions on pattern analysis and machine intelligence*, 35(8): 1798–1828, 2013.
- Berner, C., Brockman, G., Chan, B., Cheung, V., Debiak, P., Dennison, C., Farhi, D., Fischer, Q., Hashme, S., Hesse, C., et al. Dota 2 with large scale deep reinforcement learning. *arXiv preprint arXiv:1912.06680*, 2019.
- Brockman, G., Cheung, V., Pettersson, L., Schneider, J., Schulman, J., Tang, J., and Zaremba, W. Openai gym. *arXiv preprint arXiv:1606.01540*, 2016.

- Catto, E. Box2D, 2006. URL <https://box2d.org/>.
- Chevalier-Boisvert, M. Minimalistic gridworld environment (MiniGrid), 2021. URL <https://github.com/maximecb/gym-minigrid>.
- Cobbe, K., Hesse, C., Hilton, J., and Schulman, J. Leveraging procedural generation to benchmark reinforcement learning. *arXiv preprint arXiv:1912.01588*, 2019.
- Côté, M.-A., Kádár, A., Yuan, X., Kybartas, B., Barnes, T., Fine, E., Moore, J., Hausknecht, M., Asri, L. E., Adada, M., et al. Textworld: A learning environment for text-based games. In *Workshop on Computer Games*, pp. 41–75. Springer, 2018.
- Dietterich, T., Trimponias, G., and Chen, Z. Discovering and removing exogenous state variables and rewards for reinforcement learning. In *International Conference on Machine Learning*, pp. 1262–1270. PMLR, 2018.
- Dosovitskiy, A., Ros, G., Codevilla, F., Lopez, A., and Koltun, V. Carla: An open urban driving simulator. In *Conference on robot learning*, pp. 1–16. PMLR, 2017.
- Dulac-Arnold, G., Mankowitz, D., and Hester, T. Challenges of real-world reinforcement learning. *arXiv preprint arXiv:1904.12901*, 2019.
- Erez, T., Tassa, Y., and Todorov, E. Simulation tools for model-based robotics: Comparison of bullet, havok, mujoco, ode and physx. In *2015 IEEE international conference on robotics and automation (ICRA)*, pp. 4397–4404. IEEE, 2015.
- Fan, L., Wang, G., Huang, D.-A., Yu, Z., Fei-Fei, L., Zhu, Y., and Anandkumar, A. Secant: Self-expert cloning for zero-shot generalization of visual policies. *arXiv preprint arXiv:2106.09678*, 2021.
- Finn, C., Yu, T., Fu, J., Abbeel, P., and Levine, S. Generalizing skills with semi-supervised reinforcement learning. *arXiv preprint arXiv:1612.00429*, 2016.
- Flamary, R., Courty, N., Gramfort, A., Alaya, M. Z., Boissunon, A., Chambon, S., Chapel, L., Corenflos, A., Fatras, K., Fournier, N., Gautheron, L., Gayraud, N. T., Janati, H., Rakotomamonjy, A., Redko, I., Rolet, A., Schutz, A., Seguy, V., Sutherland, D. J., Tavenard, R., Tong, A., and Vayer, T. Pot: Python optimal transport. *Journal of Machine Learning Research*, 22(78):1–8, 2021. URL <http://jmlr.org/papers/v22/20-451.html>.
- Ghosh, D., Rahme, J., Kumar, A., Zhang, A., Adams, R. P., and Levine, S. Why generalization in rl is difficult: Epistemic pomdps and implicit partial observability. *Advances in Neural Information Processing Systems*, 34, 2021.
- Gretton, A., Borgwardt, K. M., Rasch, M. J., Schölkopf, B., and Smola, A. A kernel two-sample test. *The Journal of Machine Learning Research*, 13(1):723–773, 2012.
- Gupta, A., Mendonca, R., Liu, Y., Abbeel, P., and Levine, S. Meta-reinforcement learning of structured exploration strategies. *Advances in neural information processing systems*, 31, 2018.
- Hafner, D. Benchmarking the spectrum of agent capabilities. *arXiv preprint arXiv:2109.06780*, 2021.
- Hafner, D., Lillicrap, T., Norouzi, M., and Ba, J. Mastering atari with discrete world models. *arXiv preprint arXiv:2010.02193*, 2020.
- Hessel, M., Modayil, J., Van Hasselt, H., Schaul, T., Ostrovski, G., Dabney, W., Horgan, D., Piot, B., Azar, M., and Silver, D. Rainbow: Combining improvements in deep reinforcement learning. In *Thirty-second AAAI conference on artificial intelligence*, 2018.
- Hjelm, R. D., Fedorov, A., Lavoie-Marchildon, S., Grewal, K., Bachman, P., Trischler, A., and Bengio, Y. Learning deep representations by mutual information estimation and maximization. *arXiv preprint arXiv:1808.06670*, 2018.
- Hussein, A., Gaber, M. M., Elyan, E., and Jayne, C. Imitation learning: A survey of learning methods. *ACM Computing Surveys (CSUR)*, 50(2):1–35, 2017.
- Ibarz, J., Tan, J., Finn, C., Kalakrishnan, M., Pastor, P., and Levine, S. How to train your robot with deep reinforcement learning: lessons we have learned. *The International Journal of Robotics Research*, 40(4-5):698–721, 2021.
- Jaiswal, A., Babu, A. R., Zadeh, M. Z., Banerjee, D., and Makedon, F. A survey on contrastive self-supervised learning. *Technologies*, 9(1):2, 2021.
- Johnson, M., Hofmann, K., Hutton, T., and Bignell, D. The Malmo platform for artificial intelligence experimentation. In *IJCAI*, 2016.
- Juliani, A., Khalifa, A., Berges, V.-P., Harper, J., Teng, E., Henry, H., Crespi, A., Togelius, J., and Lange, D. Obstacle tower: A generalization challenge in vision, control, and planning. In *IJCAI*, 2019.
- Kahn, G., Villafior, A., Ding, B., Abbeel, P., and Levine, S. Self-supervised deep reinforcement learning with generalized computation graphs for robot navigation. In *2018 IEEE International Conference on Robotics and Automation (ICRA)*, pp. 5129–5136. IEEE, 2018.
- Ke, N. R., Didolkar, A., Mittal, S., Goyal, A., Lajoie, G., Bauer, S., Rezende, D., Bengio, Y., Mozer, M., and

- Pal, C. Systematic evaluation of causal discovery in visual model based reinforcement learning. *arXiv preprint arXiv:2107.00848*, 2021.
- Kendall, A., Hawke, J., Janz, D., Mazur, P., Reda, D., Allen, J.-M., Lam, V.-D., Bewley, A., and Shah, A. Learning to drive in a day. In *2019 International Conference on Robotics and Automation (ICRA)*, pp. 8248–8254. IEEE, 2019.
- Kingma, D. P. and Welling, M. Auto-encoding variational bayes. *arXiv preprint arXiv:1312.6114*, 2013.
- Kirk, R., Zhang, A., Grefenstette, E., and Rocktäschel, T. A survey of generalisation in deep reinforcement learning. *arXiv preprint arXiv:2111.09794*, 2022.
- Kolve, E., Mottaghi, R., Han, W., Vanderbilt, E., Weihs, L., Herrasti, A., Gordon, D., Zhu, Y., Gupta, A., and Farhadi, A. Ai2-thor: An interactive 3d environment for visual ai. *arXiv preprint arXiv:1712.05474*, 2017.
- Kormushev, P., Calinon, S., and Caldwell, D. G. Reinforcement learning in robotics: Applications and real-world challenges. *Robotics*, 2(3):122–148, 2013.
- Küttler, H., Nardelli, N., Miller, A. H., Raileanu, R., Selvatici, M., Grefenstette, E., and Rocktäschel, T. The nethack learning environment. *arXiv preprint arXiv:2006.13760*, 2020.
- Laskin, M., Srinivas, A., and Abbeel, P. Curl: Contrastive unsupervised representations for reinforcement learning. In *International Conference on Machine Learning*, pp. 5639–5650. PMLR, 2020.
- Levine, S., Finn, C., Darrell, T., and Abbeel, P. End-to-end training of deep visuomotor policies. *The Journal of Machine Learning Research*, 17(1):1334–1373, 2016.
- Lyle, C., Rowland, M., Ostrovski, G., and Dabney, W. On the effect of auxiliary tasks on representation dynamics. In *International Conference on Artificial Intelligence and Statistics*, pp. 1–9. PMLR, 2021.
- Mazouze, B., Tachet des Combes, R., Doan, T. L., Bachman, P., and Hjelm, R. D. Deep reinforcement and infomax learning. *Advances in Neural Information Processing Systems*, 33:3686–3698, 2020.
- Mazouze, B., Ahmed, A. M., MacAlpine, P., Hjelm, R. D., and Kolobov, A. Cross-trajectory representation learning for zero-shot generalization in rl. *arXiv preprint arXiv:2106.02193*, 2021.
- McDermott, D., Ghallab, M., Howe, A., Knoblock, C., Ram, A., Veloso, M., Weld, D., and Wilkins, D. PDDL—the planning domain definition language, 1998.
- Packer, C., Gao, K., Kos, J., Krähenbühl, P., Koltun, V., and Song, D. Assessing generalization in deep reinforcement learning. *arXiv preprint arXiv:1810.12282*, 2018.
- Panofsky, W. K. and Phillips, M. *Classical electricity and magnetism*. Courier Corporation, 2005.
- Poole, B., Ozair, S., Van Den Oord, A., Alemi, A., and Tucker, G. On variational bounds of mutual information. In *International Conference on Machine Learning*, pp. 5171–5180. PMLR, 2019.
- Rajan, R., Diaz, J. L. B., Guttikonda, S., Ferreira, F., Biedenkapp, A., von Hartz, J. O., and Hutter, F. Mdp playground: A design and debug testbed for reinforcement learning. *arXiv preprint arXiv:1909.07750*, 2019.
- Rigamonti, R., Brown, M. A., and Lepetit, V. Are sparse representations really relevant for image classification? In *CVPR 2011*, pp. 1545–1552. IEEE, 2011.
- Rüschendorf, L. The wasserstein distance and approximation theorems. *Probability Theory and Related Fields*, 70(1):117–129, 1985.
- Sanner, S. Relational dynamic influence diagram language (rddl): Language description, 2010.
- Savva, M., Kadian, A., Maksymets, O., Zhao, Y., Wijmans, E., Jain, B., Straub, J., Liu, J., Koltun, V., Malik, J., et al. Habitat: A platform for embodied ai research. In *Proceedings of the IEEE/CVF International Conference on Computer Vision*, pp. 9339–9347, 2019.
- Schaul, T., Horgan, D., Gregor, K., and Silver, D. Universal value function approximators. In *International conference on machine learning*, pp. 1312–1320. PMLR, 2015.
- Schulman, J., Wolski, F., Dhariwal, P., Radford, A., and Klimov, O. Proximal policy optimization algorithms. *arXiv preprint arXiv:1707.06347*, 2017.
- Schwarzer, M., Anand, A., Goel, R., Hjelm, R. D., Courville, A., and Bachman, P. Data-efficient reinforcement learning with self-predictive representations. *arXiv preprint arXiv:2007.05929*, 2020.
- Schwarzer, M., Rajkumar, N., Noukhovitch, M., Anand, A., Charlin, L., Hjelm, R. D., Bachman, P., and Courville, A. C. Pretraining representations for data-efficient reinforcement learning. *Advances in Neural Information Processing Systems*, 34, 2021.
- Silver, T. and Chitnis, R. Pddl-gym: Gym environments from pddl problems. In *International Conference on Automated Planning and Scheduling (ICAPS) PRL Workshop*, 2020. URL <https://github.com/tomsilver/pddl-gym>.

- Smirnov, N. Table for estimating the goodness of fit of empirical distributions. *The annals of mathematical statistics*, 19(2):279–281, 1948.
- Song, X., Jiang, Y., Tu, S., Du, Y., and Neyshabur, B. Observational overfitting in reinforcement learning. *arXiv preprint arXiv:1912.02975*, 2019.
- Such, F. P., Madhavan, V., Liu, R., Wang, R., Castro, P. S., Li, Y., Zhi, J., Schubert, L., Bellemare, M. G., Clune, J., et al. An atari model zoo for analyzing, visualizing, and comparing deep reinforcement learning agents. *arXiv preprint arXiv:1812.07069*, 2018.
- Sutton, R. S. and Barto, A. G. *Reinforcement learning: An introduction*. MIT press, 2018.
- Sylvain, T., Petrini, L., and Hjelm, D. Locality and compositionality in zero-shot learning. *arXiv preprint arXiv:1912.12179*, 2019.
- Szegedy, C., Ioffe, S., Vanhoucke, V., and Alemi, A. A. Inception-v4, inception-resnet and the impact of residual connections on learning. In *Thirty-first AAAI conference on artificial intelligence*, 2017.
- Tan, M. and Le, Q. Efficientnet: Rethinking model scaling for convolutional neural networks. In *International conference on machine learning*, pp. 6105–6114. PMLR, 2019.
- Team, O. E. L., Stooke, A., Mahajan, A., Barros, C., Deck, C., Bauer, J., Sygnowski, J., Trebacz, M., Jaderberg, M., Mathieu, M., et al. Open-ended learning leads to generally capable agents. *arXiv preprint arXiv:2107.12808*, 2021.
- Todorov, E., Erez, T., and Tassa, Y. Mujoco: A physics engine for model-based control. In *2012 IEEE/RSJ international conference on intelligent robots and systems*, pp. 5026–5033. IEEE, 2012.
- Wang, Y., Yao, Q., Kwok, J. T., and Ni, L. M. Generalizing from a few examples: A survey on few-shot learning. *ACM computing surveys (csur)*, 53(3):1–34, 2020.
- Xian, Y., Lampert, C. H., Schiele, B., and Akata, Z. Zero-shot learning—a comprehensive evaluation of the good, the bad and the ugly. *IEEE transactions on pattern analysis and machine intelligence*, 41(9):2251–2265, 2018.
- Yarats, D., Fergus, R., Lazaric, A., and Pinto, L. Reinforcement learning with prototypical representations. In *International Conference on Machine Learning*, pp. 11920–11931. PMLR, 2021.
- Zenke, F., Poole, B., and Ganguli, S. Continual learning through synaptic intelligence. In *International Conference on Machine Learning*, pp. 3987–3995. PMLR, 2017.
- Zhang, A., McAllister, R., Calandra, R., Gal, Y., and Levine, S. Learning invariant representations for reinforcement learning without reconstruction. *arXiv preprint arXiv:2006.10742*, 2020.
- Zhao, W., Queraltà, J. P., and Westerlund, T. Sim-to-real transfer in deep reinforcement learning for robotics: a survey. In *2020 IEEE Symposium Series on Computational Intelligence (SSCI)*, pp. 737–744. IEEE, 2020.
- Zhu, H., Yu, J., Gupta, A., Shah, D., Hartikainen, K., Singh, A., Kumar, V., and Levine, S. The ingredients of real-world robotic reinforcement learning. *arXiv preprint arXiv:2004.12570*, 2020a.
- Zhu, Y., Wang, Z., Merel, J., Rusu, A., Erez, T., Cabi, S., Tunyasuvunakool, S., Kramár, J., Hadsell, R., de Freitas, N., et al. Reinforcement and imitation learning for diverse visuomotor skills. *arXiv preprint arXiv:1802.09564*, 2018.
- Zhu, Y., Wong, J., Mandlekar, A., and Martín-Martín, R. robosuite: A modular simulation framework and benchmark for robot learning. *arXiv preprint arXiv:2009.12293*, 2020b.